



Multilevel optimization of the splitter blade profile in the impeller of a centrifugal compressor

S.A. Moussavi Torshizi, A. Hajilouy Benisi* and M. Durali

School of Mechanical Engineering, Sharif University of Technology, Tehran, P.O. Box 11155/8639, Iran.

Received 31 October 2015; received in revised form 2 February 2016; accepted 2 May 2016

KEYWORDS

Centrifugal compressor;
 Optimization;
 Splitter blades;
 Blade profile;
 Incidence loss.

Abstract. In this research, multi-level optimization of the profile of the splitter blades of a turbocharger compressor is performed using genetic algorithm in order to improve its performance. Successive corrections of the profile at hub, mid-span, and shroud of the splitter blades, with the objective of decreasing the incidence losses at the leading edge and adjustment of the blade loading at the shroud, result in an impeller having improved splitter blades. The impeller flow field analysis shows that the optimization has been successful in reducing the flow leakage at the shroud region as well as the losses in the leading edge region. Although numerical simulations predict a decrease by 0.5% in pressure ratio at design point, a 2.2-point improvement in isentropic efficiency is calculated. Based on the optimization results, a new impeller is designed, manufactured, and tested on a turbocharger test bed. Experimental results support the simulation predictions on the expected improvement in performance.

© 2017 Sharif University of Technology. All rights reserved.

1. Introduction

Flow visualization in the impeller of centrifugal compressors provided a good insight into what was really occurring during the process. In the following, several evidences are presented in the literature, showing the non-conformity of the flow approaching the splitter blades, with the same profile as that of the main blades. This implies that splitter blades must be treated differently, and that there is room for design modifications and optimization.

To achieve an effective optimization, different sources of losses must be considered. To this end, different techniques have so far been implemented. Some papers have addressed this issue by performing complex experiments. For example, flow visualization studies were conducted by Fischer and Thoma [1] in a pump. Other evidences were produced by the work of

Fowler [2] about the existence of strong non-uniform flow in the impeller of centrifugal compressors. The first explicit works discussing the jet-wake model in the impeller date back to the work of Dean [3].

Beyond these, one of the most significant pieces of information about the flow in unshrouded impellers is given in the work of Eckart [4,5] by the use of laser anemometry. Later, Krain [6] confirmed these results by laser measurements on a more efficient impeller. In these works, a wake was observed at the shroud-suction side corner of the blades. But it seems that this flow configuration is not universal. The location of the jet and wake is greatly dependent on impeller shape and diffuser performance. In these works, in addition to the main stream, existence of secondary flows and deviation of the flow from the blade profile are observable. Cumpsty [7] states that it is quite common to find that the two passages divided by a splitter behave quite differently, a matter also shown by Senoo et al. [8].

CFD simulations have been widely used in the

*. Corresponding author. Tel.: +98 21 66165512
 E-mail address: hajilouy@sharif.ir (A. Hajilouy Benisi)

study of flow and optimization procedures of centrifugal compressors. The non-uniformity of flow in impellers can be observed implicitly in all works implementing such methods [9-11].

These works confirm that due to different forces exerted on the fluid during the compression process, the flows at the two sides of splitter blades are not similar. It can be concluded that these two flows must be treated differently. However, as pointed out in well known reference books discussing the design of centrifugal compressors [12,13] as well as what is really practiced in commercial products, splitter blades have the same profile as main blades, except for having the leading part truncated to decrease inlet blockage.

Here we are trying to show that this configuration is not necessarily the best and better performance can be achieved by accurate optimization of blades. To investigate this, two methods can be considered. In the first method, splitter blades optimization is performed through variation of the location of the leading edge, without altering the blade profile. Details are discussed in [14]. In the second method presented in this work, more degrees of freedom are considered for the profile of the splitter blades with the permission to alter the design in three span layers. Since the compressor casing geometry is considered as a constraint, the profile of the main blades is not changed and major dimensions of the impeller are not affected.

2. Optimization scheme

To start the optimization process, geometry of the impeller, especially blade profiles, must be available. Here, angular definition of main blades, normalized by meridional length, is used as the basic design for generating splitters. This is to find an optimized configuration near the existing profile by the perturbation method. This method will provide solutions with much similarity to the profile of main blades, thus, easing the manufacturing process.

In general, three dimensional geometry of the blades is generated using blade profiles in at least three span layers (hub, mid-span, and shroud). To define a profile, two methods can be implemented. In the first method, a β -M curve is used in which the profile is defined using blade slope versus meridional location. The second method uses the angular position (θ) of points lying on the blades versus meridional location. Here, the second way is considered. Thus, the leading edge is always located at the origin. For optimization purpose, these continuous curves must be discretized and represented by few parameters. Here, the profiles are regenerated by 5 Bezier control points. This method needs a minimum number of data for contour generation. Figure 1 shows the application of this method on hub profile of an impeller.

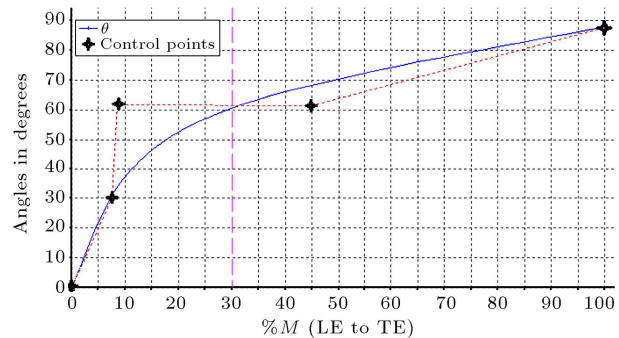


Figure 1. Angle definition of the main blades at hub span.

Generally, the location of each control point is defined by a streamwise position (M_i) and an angular position (θ_i). Considering five control points per layer and two inplane degrees of freedom for each point results in 30 optimization parameters, which imply a considerable amount of time to converge. Thus, the number of parameters must be minimized. To this end, the first two points (to the left in Figure 1), which are situated in the trimmed portion of splitter blade (vertical dash line), are fixed and others are allowed to move vertically, thus, altering the angular distribution of blades.

In the optimization loop, the values of these parameters are initially selected randomly in their allowable range (limited by the feasibility of geometry) for the first generation, and then controlled by genetic algorithm in succeeding generations. These parameters, combined by all others which are required to define the impeller geometry, are logged into a text batch file. This file is then converted to a 3D CAD file. The main blades and impeller center body are recreated by spline curves derived from the initial impeller, while splitter blades are generated using new locations of its control points as calculated by Eq. (1).

$$\theta(M) = \sum_{i=0}^4 \binom{4}{i} (1-M)^{4-i} M^i \begin{bmatrix} M_i \\ \theta_i \end{bmatrix}. \quad (1)$$

The resulting 3D geometry is meshed and prepared for CFD simulations. Finally, the compressor performance is calculated from the CFD results and fed back into the algorithm to close the optimization loop. All of these tasks are programmed to be executed sequentially until the convergence of objective function or other predefined termination rules is achieved.

Having in mind the available computing hardware, 15 generations with 15 populations each are considered. To further ease the procedure, the optimization process in each span is considered independent. In other words, altering the profile in one span will not affect the flow in others. This assumption is usually made during the design process of impellers.

Thus, 3 consecutive optimizations are performed on the impeller at spans 0, 0.5, and 0.95. The objective function is defined such that only the efficiency at the nominal working point (Eq. (2)) is maximized. Meanwhile, pressure ratio is not allowed to decrease by more than 10% of its initial value. Compensating the pressure ratio has straightforward solutions such as changing outer diameter or amount of backsweep and increasing the speed.

$$\varphi = 1 - \eta. \quad (2)$$

3. Flow simulation model

The computing tool in the optimization loop is a commercial CFD code, providing performance prediction of generated impellers. The flow domain is created and meshed using a structured hexahedral grid. An O-grid scheme for leading edge and an H-grid for trailing edge (Figure 2) are used. In the optimization of impeller geometry, due to the number of required simulations, the volute is excluded from the model. Also, only one impeller passage (including inducer and diffuser) is considered to further reduce the computational time. To capture flow details and have sufficient accuracy for wall friction, a maximum y^+ of 100 is considered. Thus, near-wall layers with 50 microns of thickness are implemented. By performing a mesh independency analysis, it is observed that a minimum mesh density of 450000 elements per passage is sufficient.

In simulations, the compressor inlet has a total pressure of 1 bar and total temperature of 300°K. The outlet of the passage is set to have a specified mass flow rate. Therefore, there is no need to assume a static pressure distribution at outlet. This item will be calculated during the solution. Also, the SST model is implemented for the turbulence modeling.

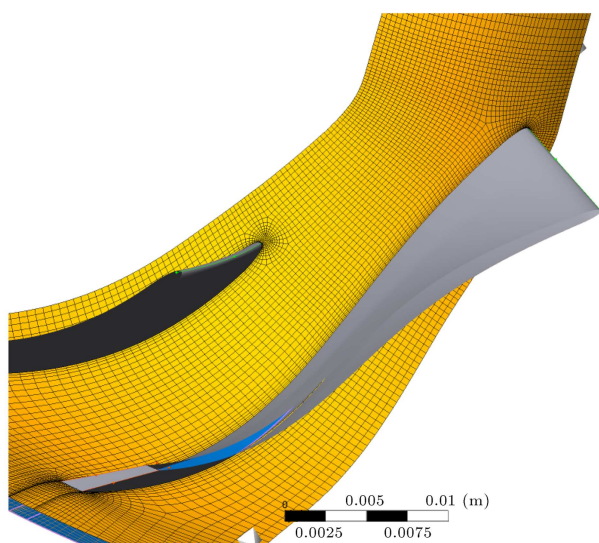


Figure 2. Generated mesh for the impeller at hub span.

Convergence criteria are set to the reduction of the root mean square of residuals for mass and momentum equations to less than 1.0E-5. Here, a virtual time step equivalent to the inverse of rotating speed is considered. Although a steady state simulation is performed, this parameter is needed to attain a fast and stable transition from initial conditions to final results. Because of non-uniformity of flow at impeller outlet, pressure ratio and efficiency are calculated by mass flow averaging of these parameters:

$$PR = \left(\iint \rho V P_0 dA / \dot{m} \right) / P_{0,in}, \quad (3)$$

$$\eta_{tt} = T_{0,in} \left(PR^{\gamma-1/\gamma} - 1 \right) / (T_{0,out} - T_{0,in}). \quad (4)$$

4. Discussion and results

The optimization procedure is implemented on the impeller of a sample centrifugal compressor of a commercial turbocharger. General specifications of the impeller are given in Table 1.

The optimized impeller design is shown in Figure 3. Detailed comparison of the impeller splitter blades reveals noticeable changes of leading edge section at hub span (Figure 4). Minor changes are also observable at shroud. In addition, the profile has moved circumferentially and, thus, is not located exactly at mid-distance between the two main blades (Figure 5). These relocations have deformed the leading edge of the splitters, causing non-radial filaments. Concerns over safety of the impeller in withstanding the centrifugal loading are checked with stress calculations by means of structural FEM simulation.

From the performance point of view, the new impeller has a maximum total to total isentropic efficiency of 87.23%, which shows 2.2 points of improvement over 85.02% of the existing impeller (both predicted by CFD calculations). At nominal working point, the new

Table 1. Specifications of the sample impeller

Parameter	Value
N	6
β_{1s}	60 degree
β_{2s}	30 degree
r_{1s}	56 mm
r_{1h}	22 mm
r_{2h}	82 mm
w_2	5.5 mm
\dot{m}_{nom}	287 g/s
PR_{nom}	2.17
ω_{nom}	92000 rpm
η_{nom}	85.02%

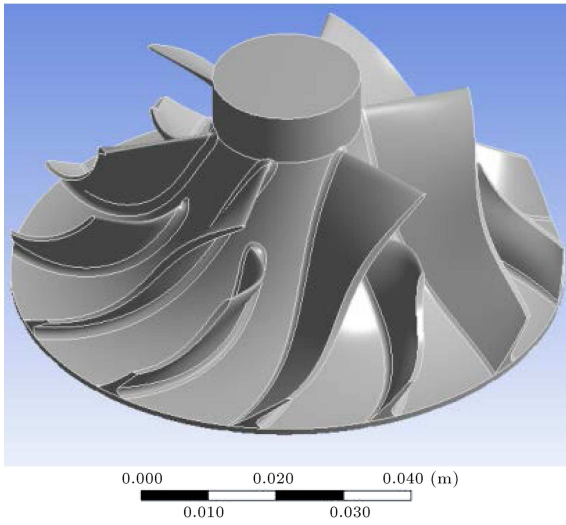


Figure 3. Optimized impeller.

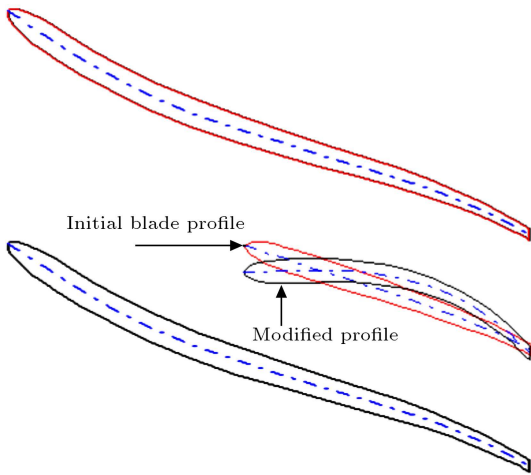


Figure 4. Comparison of splitter blade profile at hub span.

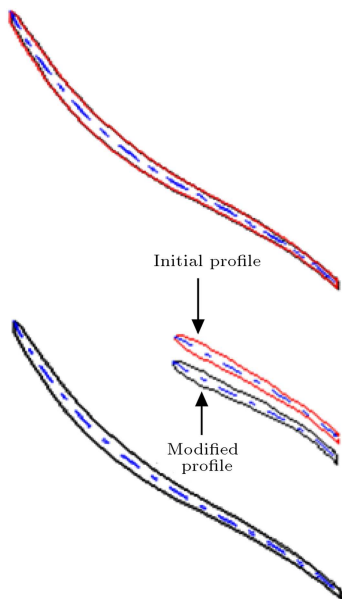


Figure 5. Profile comparison at shroud span.

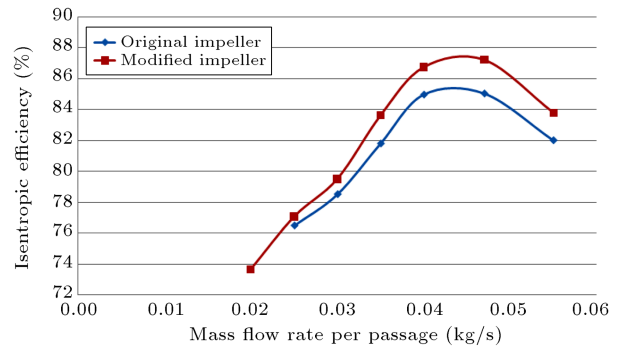


Figure 6. Efficiency predictions of the new and existing impellers at 92000 rpm.

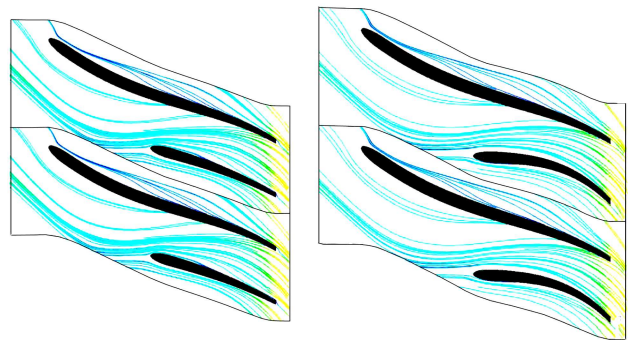


Figure 7. Streamline patterns at hub span for the existing impeller (left) and the optimized one (right).

impeller presents a pressure ratio of 2.156 compared to 2.168 of the existing impeller, which is a negligible change. Performance prediction of the new impeller and comparison with the original one at 92000 rpm is shown in Figure 6. These variations have also affected the choke margin. Simulations show that at nominal speed, the maximum mass flow rate increases from 381 g/s to 394 g/s, which is about 1.9% improvement.

To find the cause of the improvement, the flow field at different spans is examined. Figure 7 shows a blade to blade view of the streamlines at hub span. It can be seen that in the improved impeller, the splitter blades are better adapted to flow direction compared to the original blade, thus minimizing incidence losses.

The trailing edge portion has not moved. Since the blades have no direction change at the shroud, no notable variations are observed at this span.

The static pressure distributions on the blade surfaces at two spans are presented in Figures 8 and 9. At the hub span, a meaningful change in curve impellers shapes, especially at the leading edge section, is evident. As shown by the streamlines, due to a negative angle of attack in the original impeller, loading lines cross each other. That is, the suction side has higher pressure than the pressure side, which is an undesirable situation. Due to corrections made to the angle of attack, the pressure at the suction side of the blades has changed and, thus, curves are no more

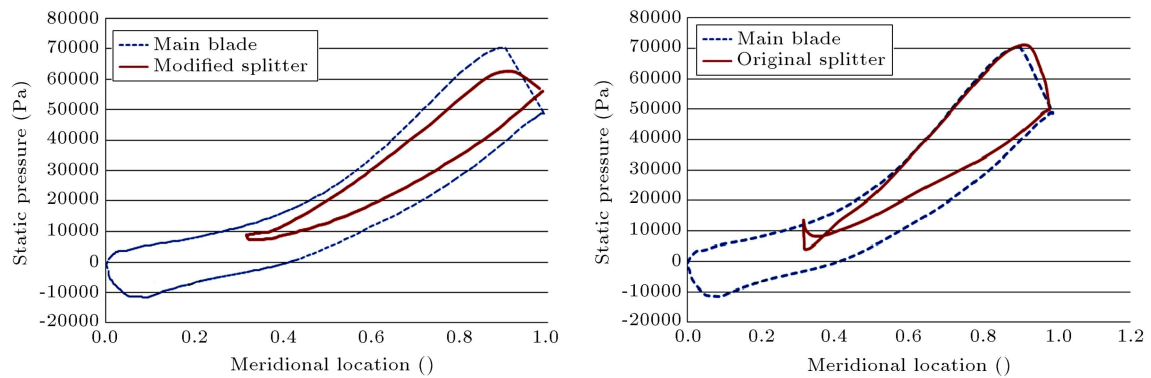


Figure 8. Blade loading at hub of the improved (left) and the original (right) .

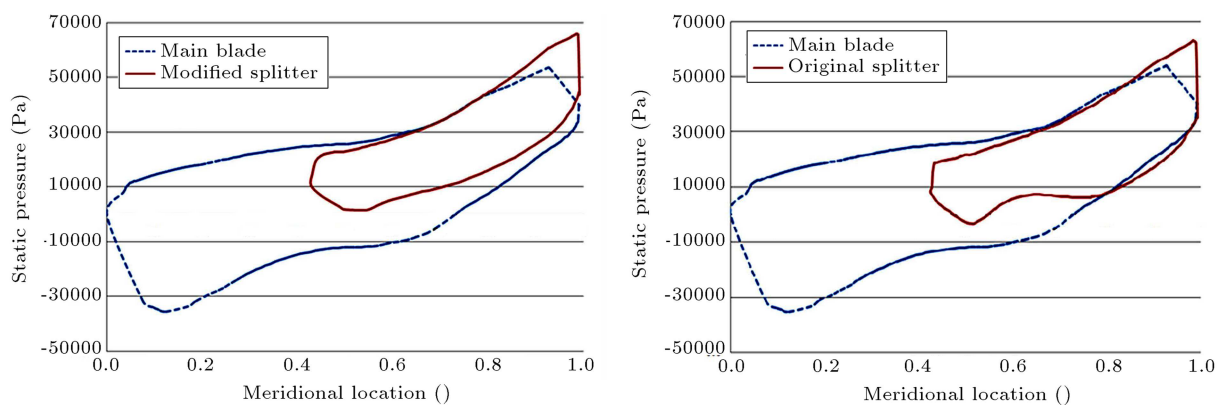


Figure 9. Blade loading at shroud of the improved (left) and the original (right) impellers.

intersecting and a normal loading curve is obtained. Loading of splitters at this span has changed up to the trailing edge and a global decrease in blade load is obvious.

At the shroud, the new loading curve presents a much smoother trend and the suction side static pressure strictly increases. Also, blade loading (pressure difference across the blade) at shroud span (span 0.9) shows a small decrease. This directly affects the tip leakage and its subsequent vortex losses. Simulations show that the leakage mass flow rate has decreased from 2.23 g/s to 1.97 g/s per blade, which presents 11.6% improvement. These decreases in blade loading are considered as the cause of the small impairment in overall pressure ratio. In all figures, loadings of the main blades have no notable change.

5. Experimental study

To validate the optimization result, the modified impeller is manufactured using Aluminum alloy 7075 T6. Stress calculations were performed using FEM analysis. The impeller body is meshed using tetrahedral elements, adaptively refined in regions of high curvature and stress concentration. Simulations are performed at 125000 rpm, maximum speed prescribed by the manufacturer. Considering 570 MPa as the ultimate

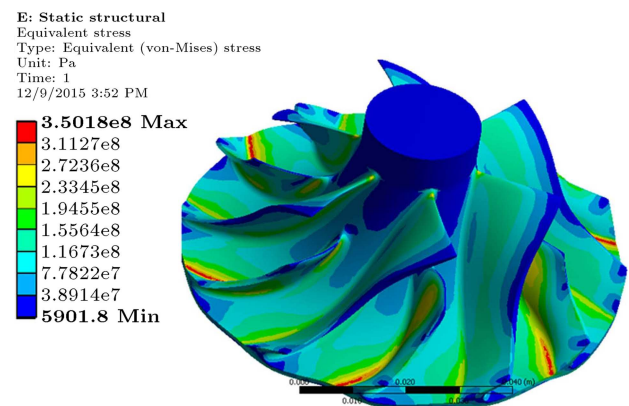


Figure 10. Stress contours of the modified impeller at 125 krpm.

strength of this alloy [15], a structural safety factor of 1.53 is achieved at the weakest point; see Figure 10.

Finally, additional geometry details such as shaft hole, fillets, seats, and tolerances are added to the model to prepare it for manufacturing. The manufactured improved impeller is shown in Figure 11.

To test the new impeller, it is mounted on a turbine shaft; see Figure 12. The modified compressor is mounted on the test bed at the Sharif University turbocharger lab. The compressor tests are performed at 50, 60, and 75 krpm with 5 operating points at



Figure 11. The manufactured impeller.



Figure 12. Modified impeller mounted on turbocharger shaft.

each speed several times with the new and existing impeller. Mass flow rates of compressor and turbine are accurately controlled with electro-pneumatic valves. Schematic of lab equipment is shown in Figure 13. Total pressure is sampled with Pitot tubes and measured with pressure transducers at compressor inlet and outlet. Total temperatures are measured by K-type thermocouples. A fiber optic sensor is used to measure the shaft speed. Compressor mass flow rate is measured with a bell mouth.

Some experimental results are shown in Figures 14

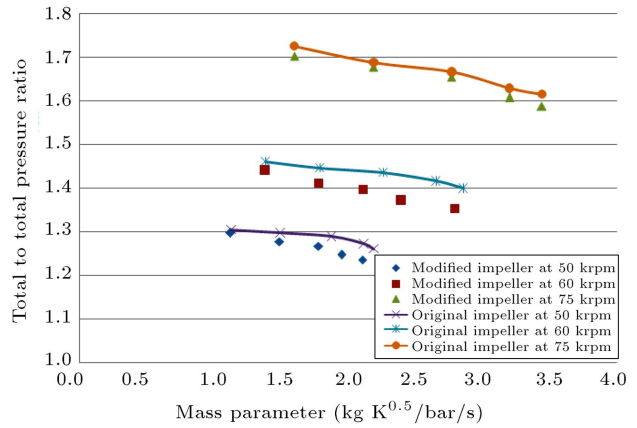


Figure 14. Experimental pressure ratio of the new and existing compressors.

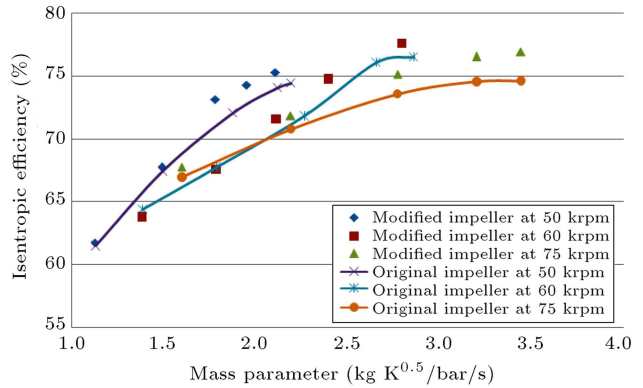


Figure 15. Experimental efficiency of the new and existing compressors.

and 15. The modified impeller performs with higher efficiency and lower pressure ratio, as expected. The maximum decrease in pressure ratio can be observed at 60 krpm by an amount of 3%. This deviation decreases at higher speeds as well as lower mass flow rates. The efficiencies of the compressors are compared in Figure 15. At low mass flow rates, compressors behave almost in the same manner. But, at higher mass flow rates, especially at higher speeds, advantage of

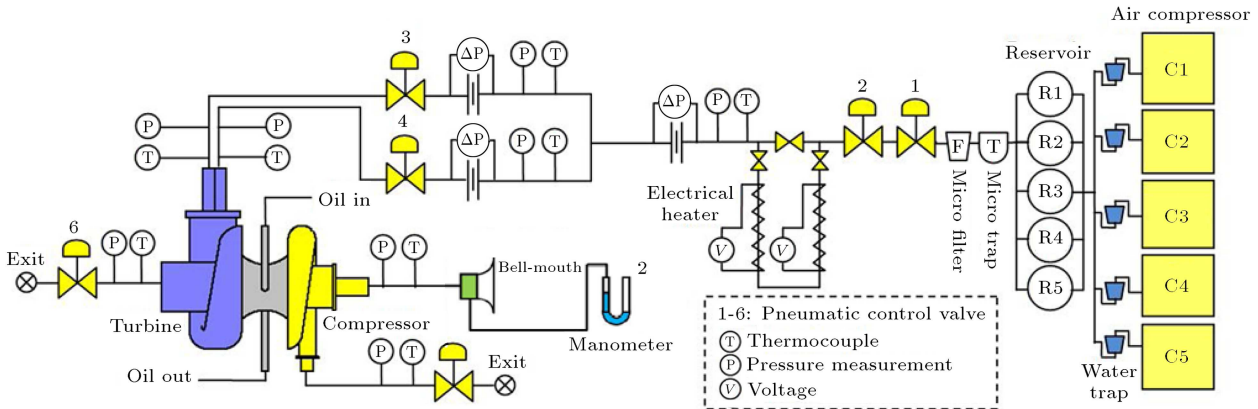


Figure 13. Schematic of turbocharger laboratory.

the new compressor is more pronounced. At 75 krpm, a maximum increase of 2.3 points in efficiency is observed. In general, with the modified impeller, better performance of the compressor is notable at all speeds and mass flow rates. Thus, the improvement is not restricted to specific working conditions, which is essential for a turbocharger.

6. Conclusion

In this research, improvements on the impeller of a turbocharger compressor were performed by altering the design of the splitter blades. This was done by redefining their profiles by Bezier control points and finding the best configuration by implementing three consecutive optimizations at hub, mid-span, and shroud sections. Structural analysis was performed on the new geometry to assure integrity and structural safety of the modified impeller. The impeller was manufactured and tested on a turbocharger test rig. Experiments confirm an increase by 2.3 points in efficiency at 75000 rpm. Precise examination of flow fields from numerical simulations of the new impeller revealed a decrease in incidence loss at the leading edge of splitter blades, especially at hub span, compared to the original impeller. Also, a decrease in leakage at the shroud region due to loading moderation is identified as the second cause of improvement. The results show that impellers with a state of the art design have room for more modifications.

Acknowledgement

The authors gratefully acknowledge the financial support of the research and technology office and technical assistance of the turbocharger laboratory staff of Sharif University of Technology.

Nomenclature

A	Area (m^2)
M	Meridional position ()
\dot{m}	Mass flow rate (g/s)
N	Number of blades ()
PR	Pressure Ratio ()
r	Radius (mm)
T	Temperature (K)
V	Velocity (m/s)
w	Passage width (mm)
β	Blade angle (degree)
η	Isentropic efficiency ()
φ	Objective function ()

ρ	Density (kg/m^3)
θ	Profile angle (degree)
ω	Speed (rpm)

Subscripts

0	Stagnation conditions
1	Compressor inlet
2	Compressor outlet
h	Hub
s	Shroud

References

1. Fisher, K. and Thoma, D. "Investigation of the flow condition in a centrifugal pump", *Transaction ASME HYD*, **54**(8), pp. 141-155 (1932).
2. Fowler, H.S. "The distribution and stability of flow in rotating channel", *Trans ASME; J. of Engineering for Power*, **90**(3), pp. 229-235 (1968).
3. Dean, R.C. "On the unresolved fluid dynamics of the centrifugal compressor", *Advanced Centrifugal Compressors, ASME*, pp. 1-55 (1971).
4. Eckart, D. "Detailed flow investigation within a high speed centrifugal compressor impeller", *J. Fluids Engineering*, **98**(3), pp. 390-399 (1976).
5. Eckart, D. "Flow field analysis of radial and backswept centrifugal compressor impeller. Part 1: Flow measurement using a laser velocimeter", *25th ASME Gas Turbine Conference*, 80-GT-33 (1980).
6. Krain, H. "Swirling impeller flow", *ASME Gas Turbine Conference*, California, 87-GT-19 (1987).
7. Cumpsty, N.A, *Compressor Aerodynamics*, Longman (1999).
8. Senoo, Y., Hayami, H., Kinoshita, Y. and Yamasaki, H. "Experimental study on flow in a supersonic centrifugal impeller", *J. Eng. Power*, **101**(1), pp. 32-39 (1979).
9. Masanao, K. and Hoshio, T. "Numerical investigation of influence of tip leakage flow on secondary flow in transonic centrifugal compressor at design condition", *Journal of Thermal Science*, **24**(2), pp. 117-122 (2015).
10. Taghavi-Zenouz, R. and Solki, E. "Centrifugal compressor performance assessment under different impeller tip clearance sizes from far to near stall conditions", *Mechanics & Industry*, **15**, pp. 253-265 (2014).
11. Shuai, G., Fei, D., Hui, T., Seng, C.L. and SinYip, M. "Multi-objective optimization for centrifugal compressor of miniturbojet engine", *Aerospace Science and Technology*, **39**, pp. 414-425 (2014).
12. Japikse, D., *Centrifugal Compressor Design and Performance*, Concepts Eti (1996).
13. Wilson, D., *The Design of High-Efficiency Turbomachinery and Gas Turbines*, Prentice Hall (1998).

14. Moussavi, S.A., Hajilouy, A. and Durali, M. "Optimization of splitter leading edge location for performance improvement of centrifugal compressors", Submitted to *Journal of Engineering for Gas Turbine and Power*, ASME (2016).
15. Joseph, R.D., *ASM Specialty Handbook: Aluminum and Aluminum Alloys*, ASM International (1993).

Biographies

Seyed Abolfazl Moussavi Torshizi received his BS (2002) and MS degrees (2006) in Mechanical Engineering with a minor in Applied Design. He is currently PhD student at Sharif University in the field of Turbomachines. His studies are mainly focused on the aerodynamic and structural design and optimization of centrifugal compressors. He has also been involved in the design and implementation of MegaWatt class wind turbine blades, since 2009.

Ali Hajilouy-Benisi received his PhD degree from Mechanical Engineering Department of Imperial College at the University of London, in 1993. He was a

faculty member of the Institute of Water and Energy and since 1978 has been the faculty member of the School of Mechanical Engineering at Sharif University of Technology (SUT). He served as Director of the Fluid Mechanics Lab (1993-1995), Founder and Director of the Turbocharger Lab (1993), Turbocharging Lab (2000), and Gas Turbine Lab (2008), in the School of Mechanical Engineering of Sharif University of Technology. His research interests are experimental and theoretical investigations of turbochargers, turbocharging, and gas turbines.

Mohammad Durali is a Professor in Mechanical Engineering Department at Sharif University of Technology. He received a BSc degree in Mechanical Engineering from Sharif University, MS, and PhD degrees in the same field from Aero and Astro Department of MIT, in 1980. His research interests are design and automation, system dynamics, and propulsion. He is currently the Head of the Center for System Design and Automation, and Creativity Lab. He has done numerous industrial design and manufacturing projects.